Higher-order Turbulence Products of Velocity and Temperature for Adverse Pressure Gradient Boundary Layer Flows

Dae Seong Kim and Bruce R. White
Department of Mechanical & Aeronautical Engineering,
University of California at Davis
One Shields Avenue, Davis, CA 95616-5294

Alberto Ayala
Department of Mechanical and Aerospace Engineering
West Virginia University
P.O. Box 6106, Morgantown, WV 26506-6106

Nader Bagheri
Department of Mechanical Engineering
California Maritime Academy, The California State University
P.O. Box 1392, Vallejo, CA 94590-0644

ABSTRACT

Higher-order turbulent products of momentum and temperature are experimentally presented for heated boundary layers subjected to adverse pressure gradient (APG) and zero pressure gradient (ZPG) flows. Clauser's equilibrium parameter, β, was set to 1.8 for APG case and 0 for ZPG case. The temperature difference between the heated wall and free stream was held constant at 12°C. Triple wire measurements were conducted to acquire simultaneous fluctuations of the two turbulent velocity components (u' and v') and the fluctuation of temperature (T'). Findings in this study show pressure gradient effect on the higher-order products, which tend to be dependent on large scale coherent structure of the boundary layer turbulence, to enhance vertical diffusion of stress, suppress stream-wise transport of stress, and increase structure sizes.

INTRODUCTION

It is known that local Reynolds number, wall-shear stress, surface roughness, and boundary layer thickness are important parameters of structure for turbulent boundary layers. Pressure gradient has been also noted as one of the parameters affecting on the coherent structure in turbulent boundary layers. Generally, decelerating flows subjected to an adverse pressure gradient (APG) thicken the boundary layer and complicate the flow characteristics; whereas, accelerating flows stabilize the boundary layer. The adverse pressure gradient often occurs in fluid flow along solid surface and may become an important issue for machinery design and maintenance due to its effect on separation and deceleration of flow. Additionally, complete structure measurements of APG flows can provide benchmark data for development of numerical turbulent models.

Kline *et al*. (1967) and Lian (1990) observed the coherent structures of TBL in the presence of APG and compared the shapes and movement of the streaks formed near the wall for zero-pressure-gradient flows. Valuable quantitative experiments on TBL subjected to APG condition have been conducted by Simpson *et al*. (1981), Watmuff and Westphal (1989), Nagano et al. (1991), Mislevy and Wang (1994), Ayala *et al*. (1997), Nagano *et al*. (1998), and others.

In the findings presented in the above studies, the validity of law-of-the-wall was shown to be questionable under APG conditions. Measurement techniques of coherent structures in boundary layers have improved with development of testing equipment and computer hardware. However, simultaneous measurement of instantaneous velocity and temperature close to the wall is still problematic. Strong intermittence of flow regimes in a boundary layer causes additional difficulty for both measurement and analysis. Therefore, different types of approach, such as conditional sampling (Murlis et al.; 1982), have been used to filter meaningful information out of massive amounts of data. In the present investigation, statistical analysis of higher order products (triple and quadrant momentum and temperature products) were measured to study APG effect on turbulent coherent structures in the boundary layer.

EXPERIMENTAL APPARATUS AND CONDITION

An open-circuit low-speed boundary-layer wind tunnel was used in the present study. The overall length of the wind tunnel is 7.5 m, which include 3 m long by 0.3 m wide test-section. The ceiling of the wind tunnel consists of thirty-six individual Plexiglas sheets, which are used to adjust the test-section geometry for a specific APG configuration. Free-stream turbulence intensities for ZPG and APG were about 1 % and 1.5 %, respectively. A further detail description of the wind-tunnel facility can be found in Ayala *et al*. (1997).

A triple wire probe (TSI 1295BH-T1.5) was used to perform simultaneous measurements of turbulence fluctuations in normal and stream-wise flow directions including temperature fluctuations. This custom-made triple wire probe consists of a tungsten X probe and a platinum temperature wire. Detailed specifications of this sensor and its application are presented in Ayala *et al*. (1997). For all turbulent measurements, the sensor real-time sampling frequency was set to 10 kHz per channel where 60,000 data points were collected at each acquisition. Wall temperature distribution was monitored with a series of thermocouples embedded in the surface and a digital thermometer. These thermocouples were calibrated against a platinum-resistance thermometer (PRT).

In the present investigation, the adverse-pressure-gradient parameter, β, was set to 1.8 which corresponded to Clauser's (1954) data. The corresponding Reynolds number value based on the momentum-deficit thickness was about 3,800. The zero-pressure-gradient boundary layer was also measured to compare its data with APG measurements.

DATA REUDUCTION

Analog voltage outputs from two Constant Temperature Anemometer (CTA) and a Constant Current Anemometer (CCA), for velocity and temperature measurements, were descritized to digital signals by a 12-bit A/D converter. A linear calibration equation was used for the voltage signal from the CCA to reduce instantaneous temperature fluctuations (with 2% uncertainty). Because the wall surface was heated and the boundary layer was under non-isothermal condition, a correction factor had to be considered for data reduction of the CTA signal. In the present study, the general correction equation,

$$E_{correct} = E_{measured}\left(\frac{T_s - T_c}{T_s - T_t}\right)^{\frac{1}{2}} \qquad (1)$$

was applied for all CTA voltage readings before it was reduced to velocity components. In Equation (1), $E_{correct}$, $E_{measured}$, T_s, T_c, and T_t are corrected voltage, measured voltage, temperature of hot-wire, ambient temperature at calibration, and local temperature at testing, respectively. The corrected voltage was reduced to turbulent velocity by using a simple calibration technique for an X-type hot wire that calculates u and v velocity component from the sensor geometry and the effective cooling velocities. Despite yaw (or pitch) angle compensation, this simple calibration gave a reasonable uncertainty of 1.8 % at a free stream velocity reading.

In terms of third- and forth-order products, the skewness and flatness (or kurtosis) factors, Sq and Fq of specified quantity, q, are defined as

$$S_q = \frac{\overline{(q-\bar{q})^3}}{\left[\overline{(q-\bar{q})^2}\right]^{\frac{3}{2}}} \quad \text{and} \quad F_q = \frac{\overline{(q-\bar{q})^4}}{\left[\overline{(q-\bar{q})^2}\right]^2} \quad , \tag{2}$$

where the overbar denotes time average.

RESULTS AND DISCUSSION

Local mean velocity profiles for ZPG and APG conditions are shown in Figure 1. With the non-dimensional mean velocity, friction velocity (u*) was determined based on the Clauser chart method. In Figure 1, the universal law-of-the-wall equation was plotted for comparison. It was found that the presented data is in agreement with the law-of-the-wall in the logarithmic core region.

Figure 2 presents a set of the instantaneous turbulent fluctuating velocity components: u' and v', temperature fluctuation T', and two triple products of velocities and temperature at y^+ of approximately 600 from the wall. The time interval for the fluctuations shown in Figure 2 is about 0.2 seconds. It is evident that the values of triple products nominally close to zero are intermittent in character and appear to be randomly amplified in magnitude. These amplitude fluctuations are dominated by coherent turbulent structures as also observed by Nagano and Tagawa (1990) and Nagano *et al*. (1991).

The behavior of the transport of turbulent energy and of shear stress is better characterized by the triple products rather than their gradients which appear in the transport equations (Murlis et al.; 1982). Figure 3 and 4 show the effect of adverse pressure gradient on streamwise and vertical turbulent transport of Reynolds shear stress, $\overline{u'u'v'}$ and $\overline{v'u'v'}$, respectively. These figures show that vertical transport of Reynolds shear stress is enhanced; whereas, streamwise diffusion is suppressed due to the adverse pressure gradient. Figure 5 displays non-dimensional vertical turbulent transport of turbulent heat flux for zero- and adverse-pressure gradient conditions. In the region of $200 < y^+ < 1000$, Figure 5 shows that adverse pressure gradient enhances vertical diffusion of scalar flux. However, in the region of $y^+ < 200$, vertical transport of $\overline{v'T'}$ under zero-pressure-gradient condition is larger than that of the adverse-pressure-gradient condition.

According to Nagano and Tagawa (1990), the turbulent motion could be categorized in (u'-v') plane to show which flow motion plays the main role in turbulent coherent structures. They named each quadrant part in the (u'-v') plane as Q1 (u'>0, v'>0), Q2 (u'<0, v'>0), Q3 (u'<0, v'<0), and Q4 (u'>0, v'<0). The fractional contributions of each quadrant part of $\overline{u'u'v'}$ and $\overline{v'u'v'}$ for zero pressure gradient and mild adverse pressure gradient (β=1.8) are compared in

Figures 6 and 7, respectively. For both triple products in the figures, it is clear that the turbulent transport of Reynolds shear stress is dominated by Q2 and Q4 motions. In Figure 6, Q2 motion under zero pressure gradient condition has a negative slope in the region of $y^+ < 300$. However, Q2 motion in the mild adverse-pressure-gradient flow shown in Figure 6 shows a positive slope for the same y+ region. Q4 motion in APG case was similar to that of the ZPG case. This suggests that adverse pressure gradient suppresses 'ejection' motion (Nagano and Tagawa; 1990) while simultaneously slightly changing the 'sweep' motion in the wall region. In Figure 7, a similar trend of APG effect on the quadrant motion (as noted for Figure 6) is observed.

Figures 8 and 9 show the distribution of skewness and flatness factors of $\overline{u'u'v'}$, $\overline{v'u'v'}$, and $\overline{v'v'T'}$. A significant characteristic of the distribution of both skewness and flatness is an abrupt peak at y^+ of about 1000. This is where the Q2 motions have the most dominant role over the rest of quadrant motions (see Figures 6 and 7). In general, high flatness factors correspond to a high fraction of non-turbulent flow, or in other words, low intermittence levels. Consequently, Figures 8 and 9 indicate that turbulent coherent structures are not present at Y^+ greater than 1000 in the ZPG. However, in the APG case it is shown the pressure gradient suppresses the occurrence of non-turbulent flow and propagates structures in the turbulent boundary layer to greater heights and widths. Skewness factors of $\overline{u'u'v'}$ and $\overline{v'u'v'}$ show similarity of trend but sign of values while skewness and flatness of $\overline{v'u'v'}$ and $\overline{v'v'T'}$ illustrates similar characteristics. This suggests that $\overline{u'u'v'}$ and $\overline{v'u'v'}$ products are in a similar relationship to compensate each other while $\overline{v'u'v'}$ and $\overline{v'v'T'}$ are governed by same physical process.

CONCLUDING REMARK

Direct measurements of instantaneous turbulent velocities and temperature fluctuation of turbulent boundary layers subjected to pressure gradients have been made. Results show the effect of adverse pressure gradient on the characteristics of higher-order turbulence products. The results was summarized as follows: i) adverse-pressure-gradient flow enhances vertical diffusion of turbulent shear stress while suppressing stream-wise transport of turbulent stress; ii) adverse-pressure-gradient flow affects the second-quadrant motion (so called 'ejection' motion) more than the fourth-quadrant motion ('sweep' motion); and, iii) adverse-pressure-gradient flows extend turbulent-boundary-layer structures to greater heights than ZPG heights and widths under similar conditions.

NOMENCLATURE

Fq	flatness (or kurtosis) factor of quantity q
Sq	skewness factor of quantity q
T'	scalar fluctuation component of local temperature
u'	stream-wise turbulence velocity fluctuation component
u^*	friction velocity
u^+	non-dimensional stream-wise velocity = u/u^*
v'	vertical turbulence velocity fluctuation component
y^+	normalized distance from the wall = yu^*/n
b	Clauser's equilibrium parameter

REFERENCES

1. Ayala, A., White, B.R., and Bagheri, N., "Turbulent Prandtl Number Measurements in Adverse Pressure Gradient Equilibrium Boundary Layers," 2nd International Symposium on Turbulence, Heat and Mass Transfer, Jan. 1997.

2. Clauser, F.H., "Turbulent Boundary Layers in Adverse Pressure Gradients," J. of Aero. Sci., 1954, vol.21, pp.91-108.

3. Kline, S.J., Reynolds, W.C., Schraub, F.A., and Runstadler, P.W., "The Structure of Turbulent Boundary Layers," J. Fluid Mech., Vol.30, 1967, pp. 741-773.

4. Lian, Q.X., "A Visual Study of the Coherent Structure of the Turbulent Boundary Layer in Flow with Adverse Pressure Gradient," J. Fluid Mech., Vol.215, 1990, pp.101-124.

5. Mislevy, S. and Wang, T. "The Effects of Adverse Pressure Gradients on the Momentum and Thermal Structures in Transition Boundary Layers," Tech. Report, Airforce Office of Scientific Research, Grant No. F49620-94-1-0126, 1994.

6. Murlis, J., Tsai, H.M., and Bradshaw, P., "The Structure of Turbulent Boundary Layers at Low Reynolds Number," J. Fluid Mech., 1982, Vol.122, pp.13-56.

7. Nagano, Y. and Tagawa, M., "A Structural Turbulence Model for Triple Products of Velocity and Scalar," J. Fluid Mech., 1990, Vol.215, pp.639-657.

8. Nagano, Y., Tagawa, M., and Tsuji, T., "Effects of Adverse Pressure Gradients on Mean Flows and Turbulence Statistics in a Boundary Layer," 8th Symposium on Turbulent Shear Flows, 1991, pp.2-3-1 - 2-3-6.

9. Nagano, Y., Tsuji, T., and Houra, T., "Structure of Turbulent Boundary Layer subjected to Adverse Pressure Gradient," Int. J. of Heat and Fluid Flow, 1998, Vol.19, No.5, pp.563-572.

10. Simpson, R.L., Chew, Y.T., Shivaprasad, B.G., and Shiloh, K., "The Structure of a Separating Turbulent Boundary Layer," J. Fluid Mech., Vol.113, 1981, pp.23-90.

11. Watmuff, J.H. and Westphal, R.V., "A Turbulent Boundary Layer at Low Reynolds Number with Adverse Pressure Gradient," 10th Australasian Fluid Mech. Conf., Dec. 1989.

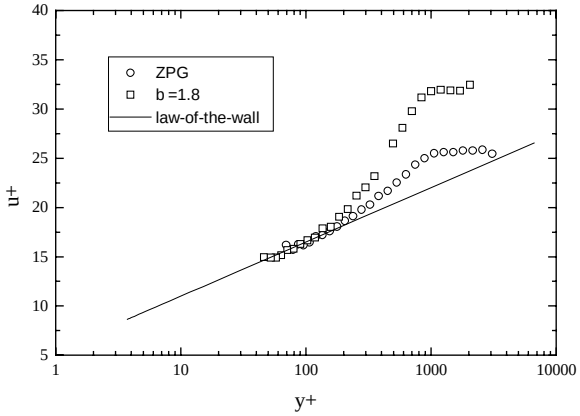

Figure 1. Non-dimensional local mean velocity profiles.

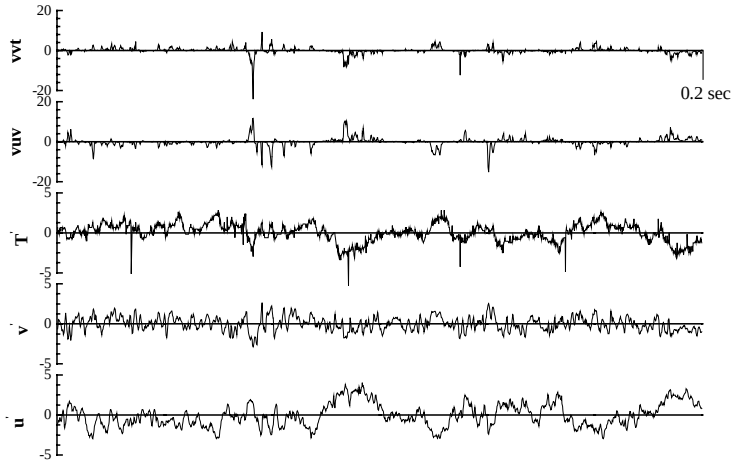

Figure 2. Instantaneous fluctuation of turbulent velocities, temperature and triple products.

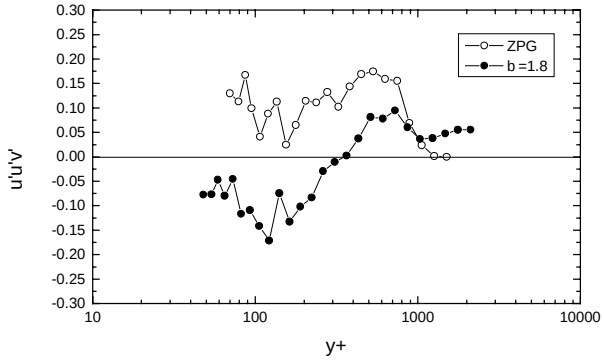

Figure 3. Comparison of $\overline{u'u'v'}$ products under ZPG and APG condition.

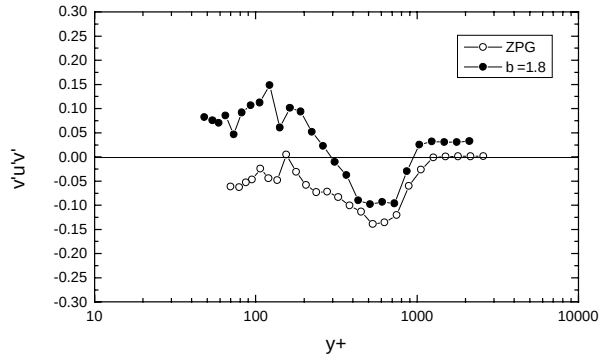

Figure 4. Comparison of $\overline{v'u'v'}$ products under ZPG and APG condition.

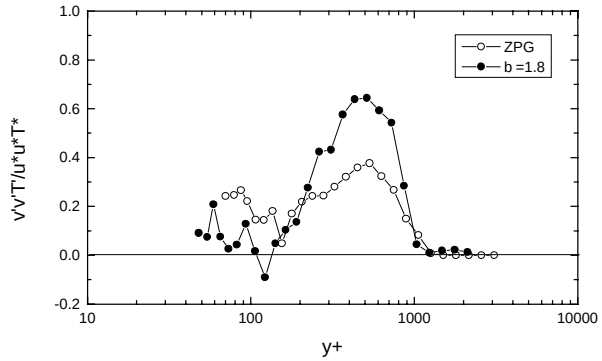

Figure 5. Comparison of non-dimensional vertical transports of scalar flux at ZPG and APG.

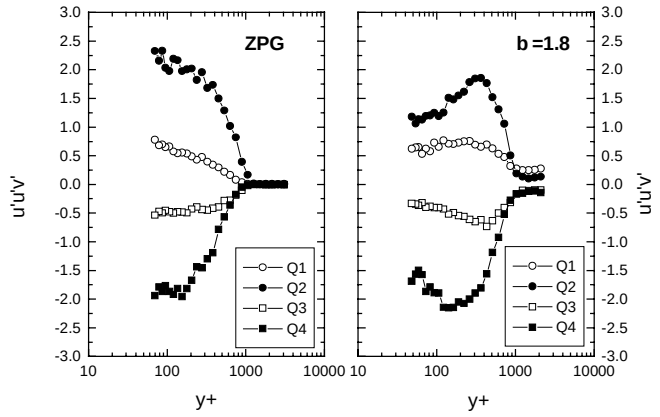

Figure 6. Comparison of fractional quadrant contributions to $\overline{u'u'v'}$ product for ZPG and APG.

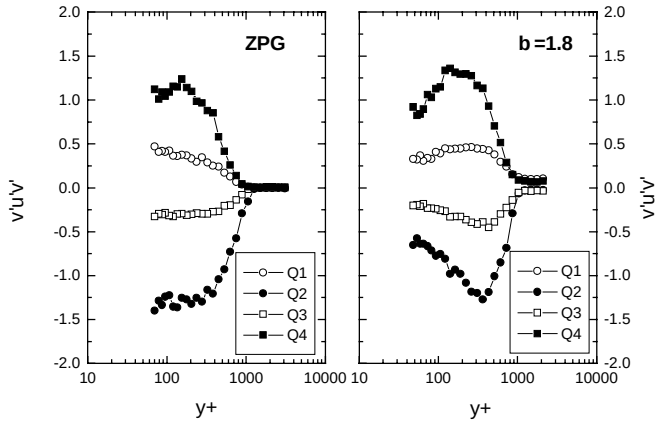

Figure 7. Comparison of fractional quadrant contributions to $\overline{v'u'v'}$ product for ZPG and APG.

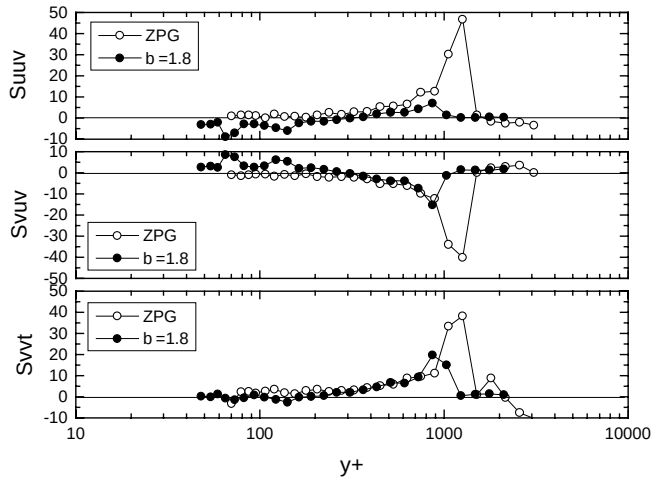

Figure 8. Skewness factors of $\overline{u'u'v'}$, $\overline{v'u'v'}$, and $\overline{v'v'T'}$ under ZPG and APG condition.

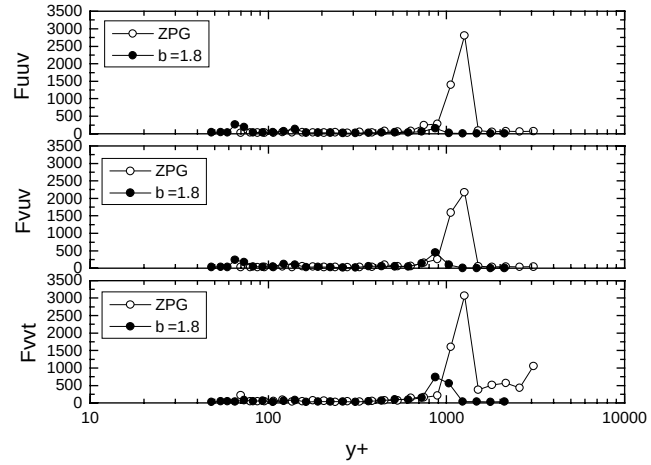

Figure 9. Flatness factors of $\overline{u'u'v'}$, $\overline{v'u'v'}$, and $\overline{v'v'T'}$ under ZPG and APG condition.